EG0800325

Preparation and Characterization of Various Activated Carbons Derived From Mixed Precursors Using Phosphoric Acid

A.A.M.Daifullah[a,*], S.E.A.Sharaf El-Deen[a], A.Elkhalafawy[a], F.A.Shehata[a] and Wagiha.H.Mahmoud[b]

(a) Department of Analytical Chemistry, Hot Lab. Center, Atomic Energy Authority.
(b) Department of Chemistry, Faculty of Science, Ain Shams University.

ABSTRACT

Rice straw (RS) and rice husk (RH), a low-cost agricultural by-products, have been used as a mixed precursor (i.e., RS mixed with RH in 1:1; 1:3 and 3:1 ratios) for the production of novel carbons using phosphoric acid as chemical activant. The raw materials were impregnated with 50% and 70% H_3PO_4 followed by activation at 500°C. The latter proved to be the most effective in producing active carbon with good adsorptive capacity. The resulting carbons were characterized by elemental analysis, infrared spectroscopy, density, SEM and S_{BET}. In general, the resulting carbons showed reasonable surface areas with mainly micropore structure. The adsorption capacity was demonstrated by the isotherms of methylene blue (MB), phenol and iodine from aqueous solution. The adsorption data was found to conform with the Langmuir equation with the concentration range studied, and the monolayer coverage was determined for each of the samples. It was found that surface area is mainly attributed to micropore volume so that phenol adsorption and iodine number correspond well with surface area determined by nitrogen adsorption.

Key Words: activated carbon; rice straw; rice husk; chemical activation, agro-residues.

INTRODUCTION

Activated carbon has widely been used for the removal of inorganic and organic pollutants from aqueous solution. In a continuing search for adsorbents, various lignocellulosic materials or agriculture wastes such as rice husks, cotton stalks, almond shells, olive stones and apricot stones were used [1-3].

Chemical activation of various carbonaceous precursors with phosphoric acid has long been known and used for the production of active carbons in industry. Many researchers have investigated the effect of precursor type, impregnation ratio and temperature of heat treatment on the properties of the resulting carbons[2-4]. It has been shown that phosphoric acid activated carbons may be obtained from lignocellulosic materials including wood [5-8], peach stone [9,10] and wheat [11].

A lot of investigations used to convert rice husks into active carbon[1,4]. Most of these reports utilized either: physical activation by steam or carbon dioxide subsequent to carbonization, or chemical activation by H_2SO_4 or zinc chloride. Chemical activation with phosphoric acid seems to be attractive due to several aspects. The process is a one-step, carbonization and activation occurring together and performed at lower temperatures (up to 500°C) and a higher yield of carbon is obtained.

In the present investigation, rice straw (RS) and rice husk (RH) were chosen as a mixed precursor
with ratios (1:1); (1:3) and (3:1) respectively. Both RH and RS composed of cellulose, hemicellulose,
lignin and ash. The mixed precursors gained some dual properties that affect the resulting carbons (porosity or surface-chemical parameters). It is aimed thus: (1) to investigate the comparative

porous structure of activated carbons derived from various RS and RH ratios by H_3PO_4 – procedure; (2) to
assess the most feasible ratio to get best carbon adsorbent with good qualities; (3) to demonstrate the

* The e-mail of the corresponding author: abdelhakim_daifullah@yahoo.com
potential capacity for removal of MB, phenol and iodine from aqueous solution; (4) to correlate the impact of precursor's mixed ratio on both surface characteristics (porosity and surface chemical nature) as well as the adsorptive capacity of carbon, consequently decitates the suitable applications.

EXPERIMENTAL

1. Materials and methods:

Rice straw (RS) and rice husk (RH) were chosen as a precursor material for preparation of 12 sorbents (Table 1). In each experiment, twenty gram of precursors was soaked in 50 or 70 vol. % H_3PO_4, in amounts sufficient to cover the all material completely, slightly agitated and left overnight. The impregnated solid was transferred to a stainless steel tube reactor fitted at one end with a perforated disc, and screw caps at both ends with narrow 10 mm tube openings to release the volatiles and tarry materials. This reactor was admitted into a sloping electric tube furnace supplied with a control for both temperature and rate of heating. The agricultural mass was heated up to 773 k gradually at rate of 50ºC/10min., and left for 2 h. Evolved gases were vented from the upper outlet to the chimney of a fume cupboard, and condensed liquids passed down though an air–cooled condenser to a water-cooled receiver. The cooled activated product was subjected to thorough washing with hot water until washings indicated a pH 6-7, then dried at 110ºC, and weighed.

2. Characterization of activated carbons:

2.1. Techniques and methods of analysis

For pH determination, 1 g of the dry, powdered carbon sample was mixed with 100 ml of bidistilled water and allowed to equilibrate for 3 days in a stoppered glass bottle. At end of this period, the pH of the carbon slurry was determined allowing 5 min. for the pH probe to equilibrate [12].

The bulk density was determined by a standard procedure by weighing a known volume of gently tapped sorbent granules[12]. The apparent density was calculated from the volume of the graduated cylinder closely packed with the powdered sample and from the sample weight.

The scanning electron microscopy (SEM: LSM T 20 JOEL, JAPAN) was additionally used to examine the surface of selected carbons. Samples for SEM examination were mounted on SEM stubs using a synthetic adhesive. No pretreatment was used for the removal of debris in order to avoid the creation of artifacts.

The elemental analysis was performed using a LECO CHNS-932 microanalysis apparatus with a VTF-900 accessory for carbon, hydrogen and nitrogen. The ash content of activated carbons was determined and calculated as described earlier[12]. Then, O% was calculated by difference.

The FTIR samples were examined as KBr discs by using Perkin Elmer 1720 FT-IR spectrometer in the 400-4000 cm^{-1} wave number range.

2.2. Adsorption of nitrogen gas:

The texture characteristics were determined by the standard N_2 adsorption isotherms, followed by their analysis to evaluate the porous parameters. Nitrogen adsorption isotherms were conducted at liquid nitrogen temperature using (Quantachrome Instruments, Model Nova 1000e series, USA). Samples were degassed at 523 K for 6 h before measurements. From the BET plots

the "monolayer equivalent surface area" (S_{BET}) was obtained, the total pore volume estimated from the volume of nitrogen adsorbed at $p/p^o = 0.95$ (Vp) and an average pore radius from $r = 2 Vp/S_{BET}$ assuming cylinderical pore dimensions[2].

2.3. Adsorption from solution:

In this concern, the uptake of iodine; phenol and methylene blue (MB) were determined from aqueous solutions. ***In case of iodine,*** 100 ml of iodine solution (0.02N) were added to previously weighed amounts (0.1- 0.5g) of activated carbon. The mixture was shaken for 2 min. and filtered. Iodine remaining in the filtrate is measured by titration against 0.02N sodium thiosulfate [13].

***In case of* phenol,** 50ml of phenol of different concentrations (50-200ppm) were shaked with 0.05g of residue for 48h. at 25ºC to construct adsorption isotherm. The adsorbent-phenol mixture is filtered and the concentration of phenol is determined by using UV-spectrophotometer at λ_{max}= 271nm[14].

***In case of* methylene blue (MB),** 50ml of MB dye of different concentrations (50-800ppm) were shaked with 0.05g of residue for 72h. The concentration of dye in the filtrate was determined by using UV-visible spectrophotometer at λ_{max}=664nm[14].

RESULTS AND DISCUSSION

1. Preparation conditions of activated carbons

Table 1 describes the preparation conditions of 12 activated carbons and illustrates some of the physicochemical characteristics. As shown in Table 1, ultimate analysis (C%; H%; N%; O%; and ash%) are described. Activated carbons normally contain inorganic components as a part of the source material, or the ash may originate from chemicals added during activation. Among the agro-residues, RH and RS have the highest ash content, 23% & 18%, respectively[15, 16, 17]. Thus, starting with (RS + RH) mixture, it was possible to produce adsorbents with varying inorganic contents between 39.9 up to 51.9%. Consequently, the ash content is more than 45.9% and only two of the 12 experimental carbons would fall below this guideline. This implies that our carbons are dual carbons. The chemisorptive properties of high ash content carbons may be advantageous in the treatment of flue gas containing acid contaminant such SO_2 and in treatment of wastewaters containing dissolved heavy metals [18].

Table (1): Preparation conditions of activated carbons

*Notation	Impregnation ratio**	H_3PO_4 Conc.	Ratio of RS:RH	Ultimate analysis				
				C%	H%	N%	Ash%	O%
$1CP_{(ex.)}$	1 : 12	50%	1 : 1	32.55	0.38	Nil	47.55	19.52
3CP	1 : 8		1 : 1	27.46	1.03	Nil	51.90	19.61
2CP	1 : 8		1 : 3	25.74	1.11	Nil	51.70	21.45
$4CP_{(ex.)}$	1 : 12		1 : 3	26.17	0.63	Nil	45.90	27.30
5CP	1 : 8		3 : 1	31.83	1.48	Nil	47.88	18.81
$6CP_{(ex.)}$	1 : 12		3 : 1	33.70	0.44	Nil	39.90	25.96
7CP	1 : 8	70%	1 : 1	33.17	0.54	Nil	50.90	15.39
$8CP_{(ex.)}$	1 : 12		1 : 1	38.15	0.40	Nil	43.99	17.46
9CP	1 : 8		3 : 1	29.59	1.22	Nil	47.96	21.23
$10CP_{(ex.)}$	1 : 12		3 : 1	34.90	1.17	Nil	45.99	17.94
11CP	1 : 8		1 : 3	23.78	0.94	Nil	47.97	27.31
$12CP_{(ex.)}$	1 : 12		1 : 3	22.20	0.57	Nil	48.96	28.27

*The subscript (ex.) indicates excess volume of H_3PO_4 (one and a half) was used under similar conditions.

** Impregnation ratio was calculated as weight of mixed precursor to volume of H_3PO_4

1.1. Characterization of active carbons:

1.1.i. Density, Yield and Ash

The Starting material with high density is desirable for the preparation of granular activated carbons (GACs). However, the density of the final products after activation depends not only on the nature of the starting material but also on activation process[19]. In this concern, as shown in Table (2), the bulk density of the resulting carbons are approximately two folds that of the original (RS+RH). These samples contain enhanced ash beside the residual phosphorous oxides, leading to the observed high apparent or bulk density and ash content. At constant temperature under the same activation procedures and as the concentration or volume of H_3PO_4 increases, the apparent or bulk density showed an irregular pattern. The maximum density was achieved with RS: RH ratio 1:3 at 50% H_3PO_4 or at 70% H_3PO_4. This indicates that not only the impregnant concentration but also the precursor ratio of (RS+RH) has significant impact on the density of the resulting carbon. i.e., the high bulk density may be referred to the high lignin content of (RS+RH). Generally, bulk density is important for activated carbon when the carbons are used in column mode. The American Water Works Association (AWWA) has set a lower limit on the bulk density at 0.25 g/ml for GACs to be of practical use [18]. The high bulk density explained by high lignin of the precursors.

Table (2): Apparent and bulk density (g/cm^3) of the prepared carbons.

Notation	H_3PO_4 Conc.	Density (g/cm^3)		Yield%	Ash%
		Apparent	Packed		
$1CP_{(ex.)}$	50%	0.313	0.416	44.22	47.55
2CP		0.303	0.513	80.40	51.70
3CP		0.250	0.500	77.90	51.90
$4CP_{(ex.)}$		0.263	0.435	79.40	45.90
5CP		0.294	0.455	68.88	47.88
$6CP_{(ex.)}$		0.263	0.357	67.45	39.90
7CP	70%	0.270	0.357	63.99	50.90
$8CP_{(ex.)}$		0.227	0.333	60.80	48.96
9CP		0.308	0.417	74.66	47.96
$10CP_{(ex.)}$		0.219	0.385	68.67	45.99
11CP		0.303	0.526	87.70	47.97
$12CP_{(ex.)}$		0.345	0.500	84.90	43.99
(RS+RH)		0.219	0.278	---	16.46

As shown in table (2), natural precursor (RS+RH) has ash content of 16.46%. However, the activated carbons that made from (RS+RH) have always higher ash content due to their high specific mineral content, especially their richness in silica [15, 16, 17]. This indicates that during the process of chemical activation using H_3PO_4 a substantial amount of carbon was consumed leading to an increase of ash content. The chemisorptive properties of high ash content carbons may be advantageous in the treatment of waste waters containing dissolved heavy metals [20].

1.1.ii. Texture properties of activated carbons

As shown in Table (3), it was clear that increasing impregnant H_3PO_4 concentration, leads to an increase in surface area and total pore volume. These results indicate that an increase in acid concentration improves pore system in the micropore range that adds much to the total surface area, total pore volume and volume enclosed in micropores. The latter is confirmed by % micropores.

Table (3): Several porous characteristics of prepared adsorbents.

Sample	H_3PO_4 %	%micropores (V_{mic}/V_px100)	S_{BET} (m^2/g)	Vp (ml/g)	Average pore radius (r), A°
$1CP_{(ex.)}$	50%	74.84%	381	0.335	17.564
2CP		77.70%	370	0.305	16.445
3CP		86.60%	381	0.277	14.541
$4CP_{(ex.)}$		69.45%	417	0.389	18.687
5CP		45.00%	360	0.409	22.705
$6CP_{(ex.)}$		56.60%	414	0.429	20.710
7CP	70%	53.70%	499	0.539	21.564
$8CP_{(ex.)}$		56.03%	512	0.552	21.554
9CP		58.90%	367	0.391	21.300
$10CP_{(ex.)}$		84.97%	571	0.415	14.537
11CP		52.83%	219	0.237	21.568
$12CP_{(ex.)}$		23.69%	248	0.261	21.069

Also, it describes the distribution of micropores to mesopores, i.e., increasing the concentration of H_3PO_4 acid leads to an increase in mesoporosity. This may be explained by the results obtained by our carbons; those prepared by 50% H_3PO_4 have % micro in the range (45 to 87%) whereas carbons
prepared by 70% H_3PO_4 have % micro in the range (24 to 85%).

The action of phosphoric acid in the activation of the lignocellulosic material may be visualized as to take place in three stages in the process of preparation: impregnation (or soaking), pyrolysis and finally leaching of the impregnant. During the course of impregnation, the acid introduce into the lignocellulose produces chemical changes and structural alterations, involving dehydration and redistribution of biopolymers possibly by partial dissolution in the acid solution together with the cleavage of linkages between the lignin and cellulose, followed by recombination reactions in which larger structural units are formed with the net result of a rigid crosslinked solid. Since H_3PO_4 intensely modifies the structure of the precursor, both the concentration of the impregnant and the conditions under which impregnation is carried out, must play important roles in the process [(21)].

In the pyrolysis stage, the introduced acid dehydrates gradually with continuation of the chemical changes involving crosslinking, water elimination and polymerization. The dehydrated impregnant have reduces tar and volatiles formation, inhibits shrinkage and collapse of the particles, and develops an extensive pore structure, with a consequential increase in the carbon yield. Finally, the third step in the preparation of active carbon, that is the washing and acid recovery, plays a very important role of porosity evolution. After carbonization, most of the activant is still in the particle and intense washing to eliminate it produces the porosity. It was found by Molina-Sabio et al. [(22)] that there is a good agreement between the volume of micropores and the volume occupied by the acid phase existing at the carbonization temperature. The entrapped polyphosphates in the final product will thus depend on its availability to leaching, and is a function of both impregnation ratio and heat treatment temperature.

Seeking for comparison, the resultant carbons were compared with a series of carbons prepared in our laboratories under similar conditions and derived from only rice husk [(23)] and another series of carbons prepared [(24)] using rice straw (cf. Table 4). The aforementioned data indicate that the resultant carbons derived from mixed precursors (RH+RS) give carbons characterized by: higher yield, low- cost, more hydrophilic, useful in various applications due to high ash content (dual sorbents); higher in density i.e. resist abrasion, capable for adsorption of small molecules with higher capacity due to their higher values of iodine number as well as these carbons have more porosity due to their higher specific surface area. Thus, the production of activated carbons from agricultural by-products serves a double purpose. First, it converts unwanted, surplus agricultural

waste, of which billions of kilograms are produced annually, to useful, value–added adsorbents. Many specific examples are found throughout the country where disposal of agricultural by – products has become a major, costly waste disposal problem. Second, activated carbons are increasingly used in water for removing organic chemicals and metals of environmental or economic concern. Consequently, production of activated carbon derived from (RS+RH) had been demonstrated to be feasible. However, activation by H_3PO_4 followed by pyrolysis at 500°C proved very effective in producing a good quality activated carbon with well-developed porosity.

Table (4): Some physicochemical properties of AC's prepared by various precursors

Parameter	H_3PO_4 Conc.	RH	RS	RH+RS
% ash	50%	23.95	32.5	51.9
% yield		62.65	32.3	77.9
Apparent density		0.234	--	0.250
bulk density		0.568	--	0.500
S_{BET}		352	236	381
V_p		0.416	0.153	0.277
Iodine #		216	--	370
% ash	70%	39.05	--	50.90
% yield		56.7		63.99
Apparent density		0.230		0.270
bulk density		0.423		0.357
S_{BET}		377		499
V_p		0.430		0.539
Iodine #		213		454

1.1.iii. Effect of Activation Conditions:

a. Burn -off

The progress of the activation may be followed by the yield, i.e., the extent of "burn-off. The extent of burn-off of the carbon material is taken as a measure of the degree of activation [25]. In this concern, Fig. (1) shows that the burn-off increase with decreasing the yield, depending on the raw material. The activated (RS+RH) has burn-off from 12 to 55% which indicates that these carbons have micropores structure except (1C) sample that has burn-off = 55% and consequently it has a mixed structure of micro and mesopores[26].

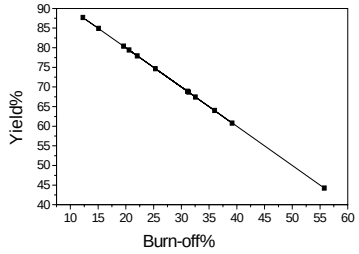

Fig. (1): Plot of burn-off vs. yield of activated carbons (1C-12C)

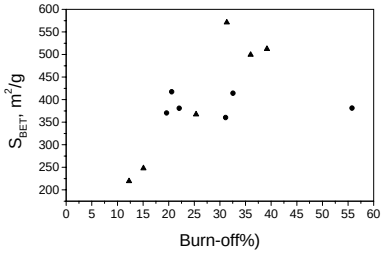

Fig. (2): Plot of burn-off Vs. S_{BET} of activated carbons (1C-12C)

This difference can be even better illustrated by the development of the inner surface area or the pore volume during the activation, Fig.(2). Accordingly, the carbons 6C and 10C samples of (3:1) raw material may be considered as a micropore with burn-off of 33% and 31% respectively.

b. Microporosity and Mesoporosity

Fig. (3) show the samples can be regarded as essentially micropores, but with a wide pore size distribution[27]. The change in micropore % and mesopore % is due to the impregnation ratio, concentration of H_3PO_4 (50% and 70%) and precursors ratios. In this concern, carbon (12C) of (1:3) raw material and 70% H_3PO_4 has the highest mesopores and the samples (3C of (1:1) at

50% H_3PO_4 and (10C) of (3:1) at 70% H_3PO_4 have the highest micropore.

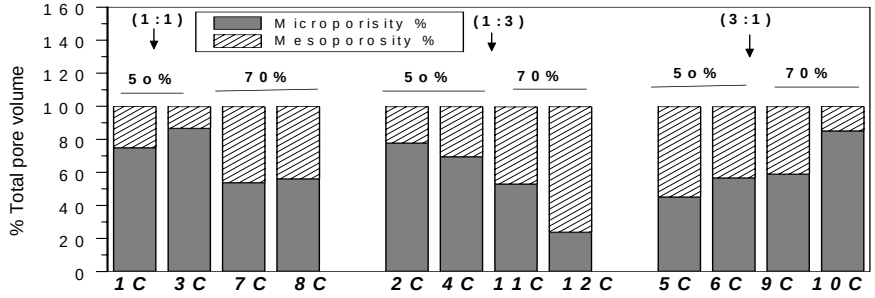

Fig. (3): Fraction precentage of carbon samples at different ratios (1:1), (1:3) and (3:1)

c- Pore size distribution:

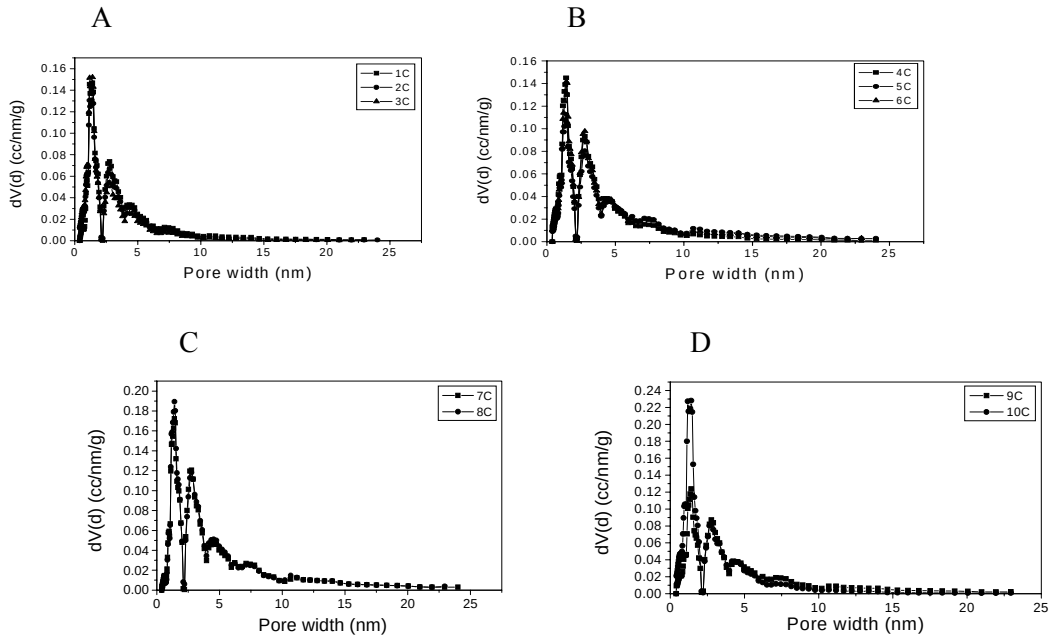

Fig. (4): DFT pore size distribution of activated carbons.

Fig. (4) show DFT pore size distribution of carbon samples. These figures indicate that the samples exhibit wide pore size distribution, from narrow micropores to wide mesopores. The peak in the region of 1nm indicate the micropore region, one model distribution of pore size is obtained in all samples. For mesopore region, a broad pore size distribution was observed with two minima at about 3nm and 5nm corresponding to the transition from pore wide accommodating one adsorbed layer to two, and two layer to three, respectively [28].

1.1.iv. Scanning Electron Microscopy (SEM):

The SEM photographs (Figs. 5-7) show progressive changes in the surface of the particles before and after activation. There are clear differences between the original mixed precursor RS:RH (1:1) as shown in Fig. 5 and lower (Fig. 6b) or the higher magnifications (Fig. 6a) as shown in sample 1C. Similar observation was clear in Figs. 7(a,b) for samples 12C.

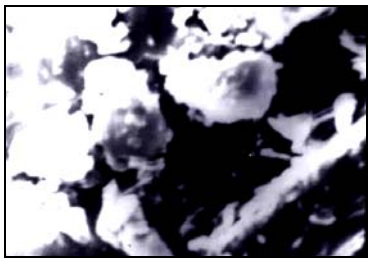

Fig. (5): SEM of raw material, the percent of RS to RH (1:1).

A(1000x) B(4000x)

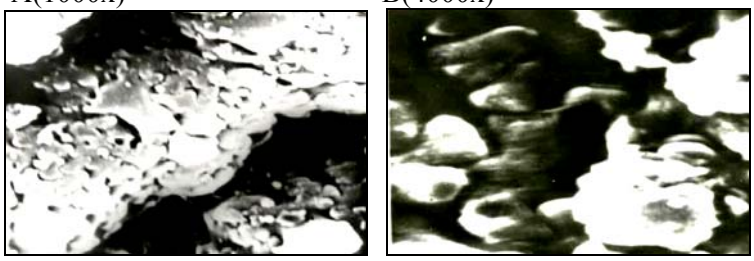

Fig. (6): Scanning electron micrograph of the sorbent 1C (A, B)

A(1000x) B(4000x)

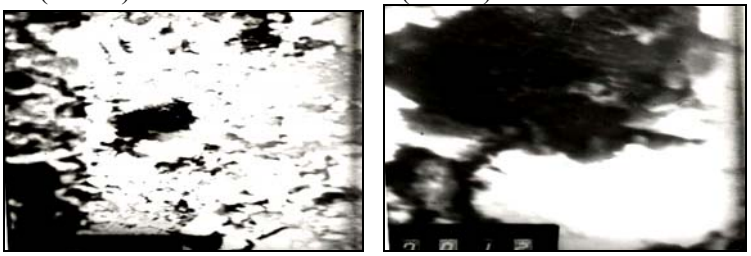

Fig. (7): Scanning electron micrograph of the sorbent 12C (A, B)

The initial morphology of the sorbent 1C (1000x) in Fig. (6A) extracted with 50% H_3PO_4 at 500ºC for 2h. shows some rods and the pores as a channel and also there are a lot of pores between the particles of the rod. As can be seen by comparing Fig. (6A) with Fig. (7A) of the sorbent 12C (1000x) extracted with 70% H_3PO_4 at 500 ºC for 2h., the particles are more agglomerated, more homogeneous and the particles are more compact. In Fig. (6B), which is the magnification of Fig. (6A), the particles are smaller than the particles shown in Fig. (7B), the percent of pores in specimen in 1C (4000x) higher than that in sample 12C (4000x) and this agree with measurements of surface area which show that S_{BET} of 1C give 381 m^2/g but for sample 12C give 248 m^2/g. in Fig. (6-A, B), the carbon percent is higher than in the sorbent 12C of Fig. (7-A, B), which C% of 1C= 32.55 but for 12C=22.2 and this mean mainly cellular structure of 1C in Fig. (6-A, B) and shown as intercellular walls, the composition of which mainly cellulose. This is in agreement with the results of the raw material (RS:RH "1:1"). From the literature, RS has mainly cellulose structure and RH has high percent of silica (which the % of SiO_2 in sample 1C=21%). In Fig. (7-A, B), the sample 12C have low surface area and this due to the raw material (RS:RH "1:3") and %SiO_2=89% which contains higher ash content and this lead to the percent of pores is small and this decrease the surface area which S_{BET} of 12C sample give 248 m^2/g.

1.1.v. Fourier-Transform Infrared Spectroscopy (FTIR):

Figs. (8, 9) shows FTIR spectra of the carbons obtained by phosphoric acid activation at two different concentrations (50%, 70%).

All spectra show 4 bands, around 3440, 2900, 1662, 1200-1000 cm^{-1}. The broad band around 3440 cm^{-1} can be assigned to the O-H stretching mode of hydroxyl groups and adsorbed water[29]. The position and asymmetry of this band at lower wave numbers indicate the presence of strong hydrogen bonds [30]. The band at 2900 cm^{-1} due to aliphatic unit as symmetric and asymmetric

stretching in C-H, CH_2 or CH_3 bonds. The two very small peaks at 1703 and 1653 cm^{-1} are usually assigned to C=O stretching vibrations of ketones, aldehydes, lactones or carboxyl groups. The weak intensity of this peak suggests that phosphoric acid activated carbons contain a small amount of carboxyl groups. The siloxane band appears around 1080 cm^{-1} due to Si-O-Si formation. Broad bands at 1300-1000 cm^{-1} are also characteristic for phosphorus and phospho carbonaceous compounds (e.g phosphates and phosphoric acid esters)[6, 31-33].

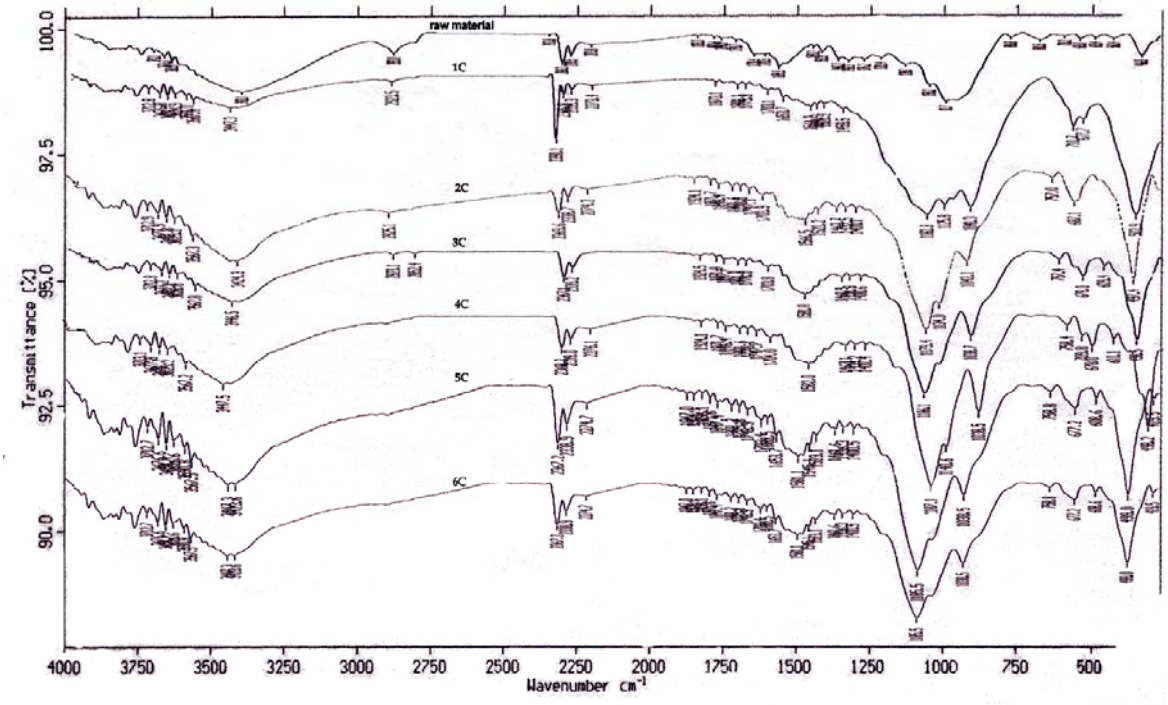

Fig. (8) FTIR spectra of the carbons (raw material and 1Cp-6Cp)

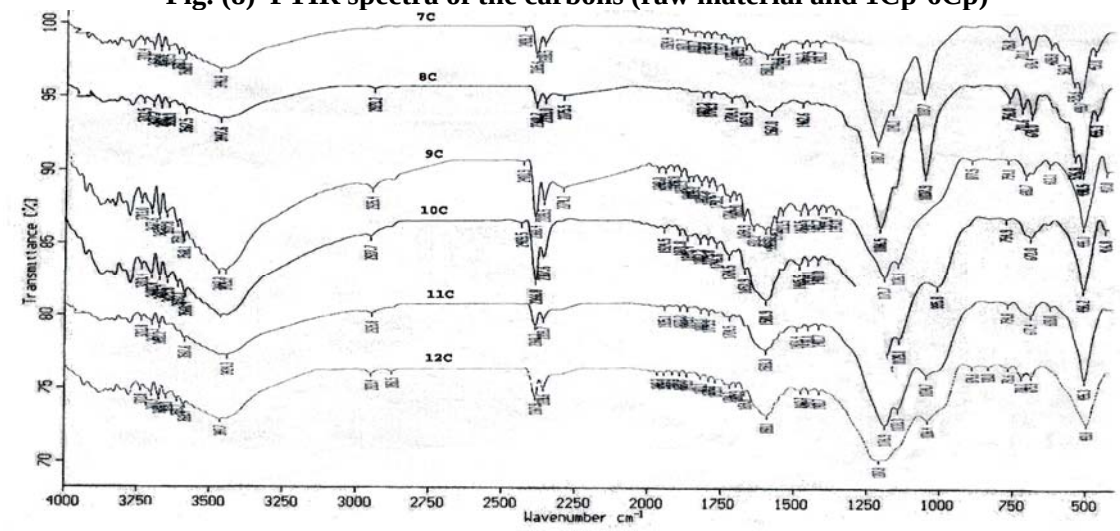

Fig. (9) FTIR spectra of the carbons (7Cp-12Cp)

1.1.vi. Adsorption from Solution:

Because of the possible practical applications of AC′s, the gas adsorption results are complemented by adsorption from solution in order to test the potential use of these carbons as general adsorbents. In practice standard testing methods are usually applied, and mentioned in producer certificates for the activated carbon so as to demonstrate its suitability in treating specific fluids and contaminants (e.g. organics, dyestuffs, metals, radioactive, ….etc). For this

purpose isotherm measurements (methylene blue; phenol and iodine) are employed in batch adsorption.

(i) Methylene Blue (MB) removal capacity:

The mesoporosity of carbon is often studied by methylene blue adsorption and this also serves as a model compound for removing organic contaminants and colored bodies from aqueous solution [(34)].

As shown in table 5 and fig.10, MB uptake is affected by different factors. It is clear that the uptake of methylene blue decreases by increasing surface area and % micropore volume but increase by increasing % mesopore volume. This indicating that the mesopore volume is more important than micropore volume in this type of adsorption. Surface area is mainly attributed to micropore volume so methylene blue adsorption negatively proportional with surface area. The methylene blue molecule has a minimum molecular cross-section of about 0.8 nm and it has been estimated that the minimum pore diameter it can enter is 1.3 nm. Therefore, it can only enter the largest micropores, but the most is likely to be adsorbed in mesopores. In contrast, the iodine molecule is greatly adsorbed due to its smaller size (0.27 nm) permitting its penetration into micropores (larger than 1 nm) [(34)]. In this concern, the surface area of (1C) at 50% H_3PO_4 is (381 m^2/g) which is lower than (8C) at 70% H_3PO_4 (512 m^2/g) but the former has MB uptake 171.8 mg/g which is grater than the latter 109.53 mg/g, this is due to (1C) has %mesoporosity of 74.87% but (8C) have %mesoporosity of 56.03%.

The high microporous carbons would make adsorption of larger molecules, as found in methylene blue. This large molecule would have difficulty entering and navigating through the micropores with the possibility that the micropores could become clogged, thereby effectively stopping further adsorption [(35)]. It is worth to mension that uptake of MB decreases as concentration of H_3PO_4 acid increases (cf. Table 5). This is due to the resultant carbons are acidic carbons (pH < 2.3) i.e., their surface have negative charge and the methylene blue has a negative charge and a repulsive forces may arise. Consequently, the uptake decreases.

Table (5): uptake of Methylene blue (MB), phenol and iodine number by activated carbons

Carbon	q^o of MB	q^o of Phenol	Iodine #
1 $CP_{(ex.)}$	171.80	26.8456	370
2 CP	130.72	32.268	390
3 CP	142.25	22.717	367
4 $CP_{(ex.)}$	120.02	28.288	450
5 CP	141.44	26.896	350
6 $CP_{(ex.)}$	109.29	27.44	441
7 CP	118.06	26.925	454
8 $CP_{(ex.)}$	109.53	56.529	500
9 CP	111.20	31.0945	374
10 $CP_{(ex.)}$	101.73	33.8066	555
11 CP	121.65	-	-
12 $CP_{(ex.)}$	179.50	-	-

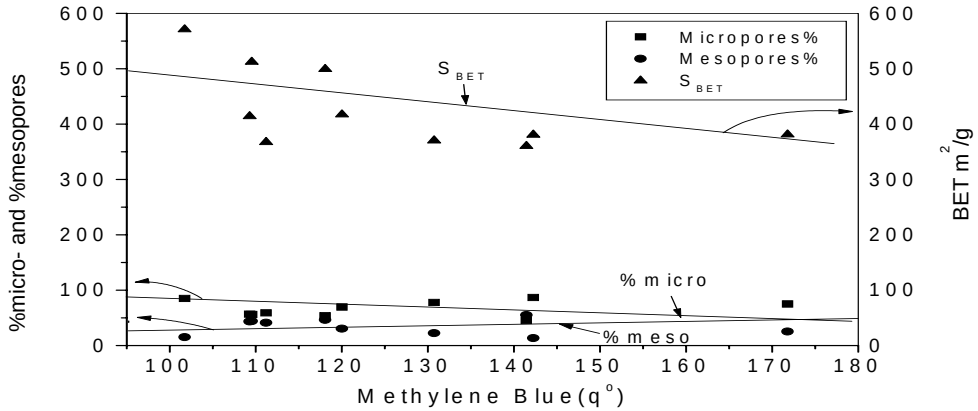

Fig. (10): Variation of methylene blue (q^o) with the porous characterstics of carbon samples with chemical activation

(ii) Phenol removal capacity:

As shown in fig.(27), it is clear that, by increasing the surface area, phenol uptake will increase. i.e, the phenol increase with increasing micropore ((% micro) as shown in the same figure. However, the higher slope is in the case of micropore than mesopore. This indicates that, phenol adsorption occurs in micropores. This observation agrees with that reported [36,37]. The data of phenol are shown in Table (5), for example, while 7C and 8C show similar values of BET-surface areas (499 and 512 m^2/g), the capacity of the former is 26.9 mg/g which is lower than the latter 56.5 mg/g. This proves that phenol adsorption does not depend exclusively on the texture of the adsorbents.

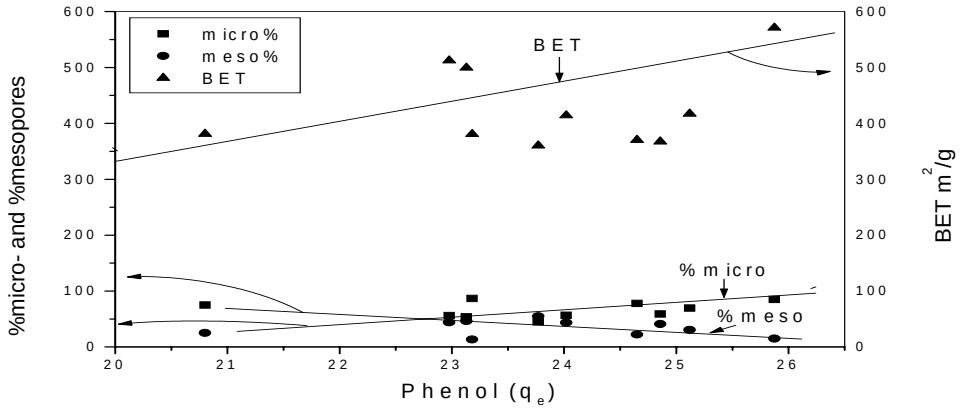

Fig. (11): Variation of phenol (q_e) with the porous characterstics of carbon samples with chemical activation

However, the phenol removal by prepared carbons affected by two factors: i) physical properties of surface (surface area, micropore volume) and ii) chemical properties of the surface imparted by either impregnation ratio or concentration of H_3PO_4. This means that phenol adsorption takes place in micropores but affected by the presence of surface functional groups because it is weak acid [3].

(iii) Iodine number:

The iodine numbers of some prepared carbons are listed in Table 5. It was clear that iodine number values are in a good agreement with surface area determined by nitrogen gas adsorption. This is due to both N_2 and I_2 are small molecules, and so can penetrate into the smallest micropores but iodine adsorption is not restricted to surface coverage unless high ratios I^-/I_2 are used [38]. However, the iodine number indicates that the number of pores larger than 1nm, through which iodine can penetrate [39], reached its maximum at carbon sample "10C" as shown in Table (5).

CONCLUSION

The production of activated carbons from mixed precursors (RS+RH) had been demonstrated to be feasible. These carbons were compared with carbons derived from either RS or RH under similar conditions of preparations. The resultant carbons characterized by : higher yield, low-cost, more polar and higher hydrophobicity, useful in various applications due to high ash content (dual sorbents); higher in density i.e. resist abrasion, capable of adsorption of small molecules with higher capacity due to their higher values of iodine number. Besides, these carbons have more porosity due to their higher specific surface area. Consequently, production of activated carbon derived from mixed precursors (RS+RH) using chemical route using H_3PO_4 at 500°C produce good quality of activated carbon with well-developed porosity.

REFERENCES

1. A.A.M. Daifullah, B.S. Girgis, H.M.H. Gad "Utilization of agro-residues (rice husk) in small waste water treatment plans", Materials letters 57 (2003) 1723- 1731.
2. A.A.M. Daifullah, B.S. Girgis "Impact of surface characteristics of activated carbon on adorption of BTEX," Colloids and Surfaces A: 214 (2003) 181 – 193.
3. A.A.M. Daifullah and B.S. Girgis, Removal of some substituted phenols by activated

carbon obtained from agricultural waste, Wat. Res., 32 (4), 1998, 1169- 1177.
4. A.A.M.Daifullah and B.S. Girgis, H.M.H.Gad, A study on the factors affecting the removal of humic acid by activated carbon prepared from biomass material, Colloids and Surfaces A: 235 (2004) 1-10.
5. W.H. Lee, P.J. Reucroft. Vapor adsorption on coal- and wood- based chemically activated carbons. I. Surface oxidation states and adsorption of H_2O. Carbon 1999; 37(I):7-14.
6. M.S. Solum, R.J. Pugmire, M. Jagtoyen, F. Derbyshire. Evolution of carbon structure in chemically activated wood. Carbon 1995;33(9):1247-54.
7. H. Benaddi, T.J. Bandosz, J. Jagiello, J.A. Schwarz, J.N. Rouzaud, D. Legras, F. Béguin. Surface functionality and porosity of activated carbons obtained from chemical activation of wood. Carbon 2000; 38:669-74.
8. I.I. Salame, T.J. Bandosz. Comparison of the surface features of two wood-based activated carbons. Ind Eng Chem Res 2000; 39:301-6.
9. J.A.F. MacDonald, D.F. Quinn. Adsorbents for methane storage made by phosphoric acid activation of peach pits. Carbon 1996; 34(9):1103-8.
10. M. Molina-Sabio, F. Caturla, F. Rodriguez-Reinoso. Influence of the atmosphere used in the carbonization of phosphoric acid impregnated peach stones. Carbon 1995; 33(8):1180-2.
11. Y. Diao, W.P. Walawender, L.T. Fan. Production of activated carbons from wheat using phosphoric acid activation. Adv. Environ Res 1999; 3(3):333-42.
12. G. Mckay. "Use of Adsorbent for the Removal of Pollutants from Wastewaters" CRC Press, New York (1996).
13. Standard test method for determination of iodine number of activated carbon, ASTM D4607-94 (ASTM), 1999).
14. A. Aygun, S. Yenisoy-Karakas, and I. Duman, Microporous and Mesoporous Mater., 66, 189-195 (2003).
15. C. L. Mantell, Industrial Carbon: Its Elemental, Adsorptive and Manufactured Forms, Second edition. D Van Nostrand Company Inc. New York. (1946).
16. W. E. Marshall, and E. T. Champagne, J. Environ. Sci. Health, A30, 241-261 (1995).
17. W. E. Marshall, and E. T. Champagne, W.J. Evans, J. Envir. Sci. and Health, A28 (9), 1977-1992(1993).
18. S. M. Yakout , Ph.D. Thesis, university of Ain Shams, Faculty of Science, Chem. Dep., 2005.
19. A. C. Lua, and J. Guo, Carbon, 38, 1089-1097 (2000).
20. E. Bayer, A. Maurer, C. J. Deyle, and M. Kutubuddin, Fresenius Envir. Bull, 4, 539-544 (1995).
21. F. Rodriguez-Reinoso, M. Molina-Sabio, Carbon 30 (1992) 1111.
22. M. Molina-Sabio, F. Rodriguez-Reinoso, F. Caturla, M.J. Sellés. Development of porosity in combined phosphoric acid carbon dioxide activation. Carbon 1996; 34(4):457-62.
23. H.H. Gad, Ph.D. Thesis, university of Mansoura, Faculty of Science, Chem. Dep., 2003.
24. W.E. Rashwan and B.S. Girgis, Adsorption, Science & Technology, 22(3), 2004, 181-194.
25. S. Manocha et al, Carbon Sci. (2002).
26. R. C. Bansal, J.B.t. Donne and F. Stoeckli. "Active Carbon", Marcel Dekker, Inc, New Yourk (1988).
27. F. Suarez-Garcia, A. Martinez-Alonso, and J. M. D. Tascon, J. Anal. And Appl. Pyrolysis, 63, 283-301 (2002).
28. S. Villar-Rodile, R. Denoye, J. Rouquero, A. Martinez-Alonso, and J. M. D. Tascon, J. Colloid and Interface Sci., 252, 169-176 (2002).
29. B. Stuart, Modern Infrared Spectroscopy, Wiley, Chichester, UK, 1996.
30. J. Zawadzki, Infrared spectroscopy in surface chemistry of carbons. In: Thrower PA. editor. Chemistry and physics of carbon. Vol. 21. New York: Marcel Dekker. 1989. pp. 147 386.

31. M. Jagtoyen, M. Thwaites, J. Stencel, B. McEnaney, F. Derbyshire. Adsorbent carbon synthesis from coals by phosphoric activation. Carbon 1992; 30(7):1089-96.
32. D.E.C. Corbridge. Infra-red analysis of phorous compounds. J Appl. Chem 1956; 6:456-65.
33. G. Socrates. Infrared characteristic group frequencies. New York, John Wiley. 1994.
34. S. Yenisoy-Karakas, A. Aygun, M. Gunes, and E. Tahtasakal, Carbon, 42, 477-484 (2004).
35. B. Pendyal, M. M. Johns, W. E. Marshall, M. Ahmedna, and R. M. Rao, Bioresource Technol., 69, 45-51 (1999).
36. C. O. Ania, J. B. Parra, and J. J. Pis, Fuel Proc. Tech., 77-78, 337-343 (2002).
37. H. Jankowska, A. Swiatkowski, D. Gelbin, K. H. Radeke, and A. Seidel, Ext. Abstr. Int. Carbon Conf. "Carbon 86" 397 (1986).
38. M. Molina-Sabio, C.S.M. De Lecea, F. Rodriguez-Reinoso, C. Puente-Ruiz And A. L. Solano, Carbon, 23(I) 91-96 (1985).
39. K. Gergova, N. Petrov, and S. Eser, Carbon, 32(4), 693 (1994).